The Canonical Transient Receptor Potential 6 Channel as a Putative Phosphatidylinositol 3,4,5-Trisphosphate-Sensitive Calcium Entry System†

Ping-Hui Tseng,‡ Ho-Pi Lin,‡ Hongzhen Hu,§ Chunbo Wang,§ Michael Xi Zhu,§ and Ching-Shih Chen*,‡

Division of Medicinal Chemistry, College of Pharmacy, and Department of Neuroscience and Center for Molecular Neurobiology, The Ohio State University, Columbus, Ohio 43210

Received April 4, 2004; Revised Manuscript Received June 15, 2004

ABSTRACT: We previously reported that phosphatidylinositol 3,4,5-trisphosphate (PIP_3), a lipid product of phosphoinositide 3-kinase (PI3K), induced Ca^{2+} influx via a noncapacitative pathway in platelets, Jurkat T cells, and RBL-2H3 mast cells. The identity of this Ca^{2+} influx system, however, remains unclear. Here, we investigate a potential link between PIP_3-sensitive Ca^{2+} entry and the canonical transient receptor potential (TRPC) channels by developing stable human embryonic kidney (HEK) 293 cell lines expressing TRPC1, TRPC3, TRPC5, and TRPC6. Two lines of evidence support TRPC6 as a putative target by which PIP_3 induces Ca^{2+} influx. First, Fura-2 fluorometric Ca^{2+} analysis shows the ability of PIP_3 to selectively stimulate $[Ca^{2+}]_i$ increase in TRPC6-expressing cells. Second, pull-down analysis indicates specific interactions between biotin-PIP_3 and TRPC6 protein. Our data indicate that PIP_3 activates store-independent Ca^{2+} entry in TRPC6 cells via a nonselective cation channel. Although the activating effect of PIP_3 on TRPC6 is reminiscent to that of 1-oleoyl-2-acetyl-*sn*-glycerol, this activation is not attributable to the diacylglycerol substructure of PIP_3 since other phosphoinositides failed to trigger Ca^{2+} responses. The PIP_3-activated Ca^{2+} entry is inhibited by known TRPC6 inhibitors such as Gd^{3+} and SKF96365 and is independent of IP_3 production. Furthermore, we demonstrated that TRPC6 overexpression or antisense downregulation significantly alters the amplitude of PIP_3- and anti-CD3-activated Ca^{2+} responses in Jurkat T cells. Consequently, the link between TRPC6 and PIP_3-mediated Ca^{2+} entry provides a framework to account for an intimate relationship between PI3K and PLCγ in initiating Ca^{2+} response to agonist stimulation in T lymphocytes.

The mammalian transient receptor potential (TRP)[1] superfamily comprises more than 20 related cation channels that are classified into three families, i.e., TRPC, TRPM, and TRPV (*1*, *2*). Despite displaying a high degree of sequence homology and structural similarity, these channels are differentially expressed in various tissues and play discrete roles in diverse physiological responses. The mechanism by which each type of TRP channel is activated underlies the molecular basis of this intriguing functional diversity. Among various putative mechanisms, it is noteworthy that activation by a phospholipase C- (PLC-) dependent pathway characterizes members of the canonical TRP (i.e., TRPC) family, designated TRPC1 through TRPC7 (*3*). Receptor-mediated stimulation of PLC leads to the production of D-*myo*-inositol 1,4,5-trisphosphate (IP_3) and diacylglycerol (DAG) via the hydrolysis of phosphatidylinositol 4,5-bisphosphate (PIP_2). This PLC pathway affects TRPC activation through a number of distinct mechanisms. For example, under certain conditions some TRPC proteins form store-operated channels (SOCs), which are activated by the release of Ca^{2+} from internal stores (*4*, *5*). In addition, DAG directly activates TRPC3 and its close relatives, TRPC6 and TRPC7, independent of IP_3 action or store depletion (*6*). Moreover, evidence indicates that TRPC activation may involve interactions with IP_3 receptors or ryanodine receptors in a manner consistent with the conformational coupling model (*7*−*9*).

Our recent studies suggest that phosphoinositide 3-kinase (PI3K) acts in concert with PLC in initiating receptor-mediated Ca^{2+} signaling in various hematopoietic cell systems including platelets, Jurkat T lymphocytes, and RBL-2H3 mast cells (*10*−*12*). Our evidence indicates that the PI3K lipid product phosphatidylinositol 3,4,5-trisphosphate (PIP_3) mediates Ca^{2+} influx through a mechanism independent of PLC activity or store depletion (*10*−*12*). It is well understood that activation of many receptor tyrosine kinase cascades leads to the membrane colocalization of PLCγ and

† This work is supported by National Institutes of Health Grants GM53448 (to C.-S.C.) and NS42183 (to M.X.Z.).

* To whom correspondence should be addressed. Tel: (614) 688-4008. Fax: (614) 688-8556. E-mail: chen.844@osu.edu.

‡ Division of Medicinal Chemistry, College of Pharmacy, The Ohio State University.

§ Department of Neuroscience and the Center for Molecular Neurobiology, The Ohio State University.

[1] Abbreviations: TRPC, canonical transient receptor potential; PI3K, phosphoinositide 3-kinase; PIP_3, phosphatidylinositol 3,4,5-trisphosphate; PIP_2, phosphatidylinositol 4,5-bisphosphate; PI, phosphatidylinositol; di-C_8, dioctanoyl; $[Ca^{2+}]_i$, intracellular Ca^{2+}; SOC, store-operated channel; HEK, human embryonic kidney; DAG, diacylglycerol; OAG, 1-oleoyl-2-acetyl-*sn*-glycerol; PLC, phospholipase C; IP_3, D-*myo*-inositol 3,4,5-trisphosphate; IP_3R, D-*myo*-inositol 3,4,5-trisphosphate receptors; biotin-PIP_3, 1-*O*-{1-*O*-[4-(*N*-biotinoylamino)octanoyl]-2-*O*-octanoyl-*sn*-glycero-3-phosphoryl}-*myo*-inositol 3,4,5-trisphosphate; biotin-PIP_2, 1-*O*-{1-*O*-[4-(*N*-biotinoylamino)octanoyl]-2-*O*-octanoyl-*sn*-glycero-3-phosphoryl}-*myo*-inositol 4,5-bisphosphate; HA, hemagglutinin; HETE, 20-hydroxyeicosatetraenoic acid.

10.1021/bi049349f CCC: $27.50
Published on Web 08/27/2004

PI3K, which use the mutual substrate PIP_2 to generate two structurally and functionally distinct second messengers, IP_3 and PIP_3. We rationalize that these two signaling molecules trigger the activation of Ca^{2+} channels at different cellular compartments, giving rise to elevated $[Ca^{2+}]_i$ required for optimal physiological responses to receptor stimulations. Consequently, the identity of the PIP_3-sensitive Ca^{2+} entry system constitutes the focus of our current studies. For the present work, we investigated a potential link between PIP_3-sensitive Ca^{2+} entry and TRPC channels, of which the rationale is multifold. First, many of the TRPC proteins are expressed in platelets, Jurkat T lymphocytes, and RBL-2H3 cells (*13*−*15*), in which PIP_3-induced Ca^{2+} entry occurs. Second, lipids such as 1-oleoyl-2-acetyl-*sn*-glycerol (OAG), 20-hydroxyeicosatetraenoic acid (HETE), epoxyeicosatrienoic acids, and PIP_2 have been demonstrated to be regulators of TRP channels (*6*, *16*−*18*), indicating a link between TRPC function and lipid mediators. Third, in addition to our studies in hematopoietic cells (*11*, *12*), a recent report described the participation of PI3K in the endothelin-1-induced activation of a SOC and a Ca^{2+}-permeable nonselective cation channel in CHO cells (*19*), suggesting cross talk between PI3K and Ca^{2+} channels in plasma membranes.

Here, we developed stable human embryonic kidney (HEK) 293 cell lines expressing TRPC1, TRPC3, TRPC5, or TRPC6 and studied the differential interaction of PIP_3 with individual TRPC proteins via two different strategies. First, we examined the Ca^{2+} influx properties of these stably transfected cell lines in response to PIP_3 stimulation. Second, we used biotinylated analogues of PIP_3 (biotin-PIP_3) and PIP_2 (biotin-PIP_2) to confirm TRPC binding by pull-down analysis. Moreover, using Jurkat T cells, we demonstrated that the amplitude of PIP_3- and, more importantly, anti-CD3-mediated Ca^{2+} response could be altered by modulating the level of TRPC6 expression. Together, these data suggest a link between TRPC6 and PIP_3-mediated Ca^{2+} response, of which the significance is at least twofold. First, this link provides a molecular framework to account for the physiological role of PI3K in the activation of leukocytes and platelets. Second, this PIP_3-sensitive Ca^{2+} channel can be pharmacologically exploited as a therapeutic target for diseases related to these blood cells.

EXPERIMENTAL PROCEDURES

Materials. 1-*O*-(1,2-Di-*O*-palmitoyl-*sn*-glycero-3-*O*-phosphoryl)-D-*myo*-inositol 3,4,5-trisphosphate (PIP_3), 1-*O*-(1,2-di-*O*-octanoyl-*sn*-glycero-3-*O*-phosphoryl)-D-*myo*-inositol 3,4,5-trisphosphate (di-C_8-PIP_3), 1-*O*-(1,2-di-*O*-palmitoyl-*sn*-glycero-3-*O*-phosphoryl)-D-*myo*-inositol 4,5-bisphosphate (PIP_2), and 1-*O*-(1,2-di-*O*-palmitoyl-*sn*-glycero-3-*O*-phosphoryl)-D-*myo*-inositol (PI) were obtained from CellSignals, Inc. (Columbus, OH). 1-*O*-{1-*O*-[4-(*N*-Biotinoylamino)octanoyl]-2-*O*-octanoyl-*sn*-glycero-3-phosphoryl}-*myo*-inositol 3,4,5-trisphosphate (biotin-PIP_3) and 1-*O*-{1-*O*-[4-(*N*-biotinoylamino)octanoyl]-2-*O*-octanoyl-*sn*-glycero-3-phosphoryl}-*myo*-inositol 4,5-bisphosphate (biotin-PIP_2) were synthesized as previously reported (*20*). Fura-2 acetoxymethyl ester (AM), SKF96365, and carbachol were purchased from Calbiochem (San Diego, CA). Rabbit anti-TRPC5 and anti-TRPC6 were purchased from Alomone Labs (Jerusalem, Israel), rabbit anti-HA antibodies and anti-type III inositol 3,4,5-trisphosphate receptors (IP_3Rs) were obtained from Santa Cruz Biotechnology (Santa Cruz, CA), and mouse monoclonal anti-actin was from ICN Biomedicals Inc. (Costa Mesa, CA). Mouse anti-human CD3 antibody was from BD Bioscience (San Diego, CA). Other chemicals or biochemical agents were purchased from Sigma (St. Louis, MO), unless otherwise specified.

Cell Culture and Transfection of TRPC Constructs. HEK293 and Jurkat T lymphocytes, purchased from American Type Culture Collection (Manassa, VA), were grown in T-75 tissue culture flasks at 37 °C in a humidified incubator (5% CO_2) in Dulbecco's modified Eagle's medium (DMEM) supplemented with 10% fetal bovine serum (FBS) and in 10% FBS-supplemented RPMI 1640 medium, respectively. Stable cell lines overexpressing HA-tagged human TRPC1 and TRPC3 were established as previously described (*21*). For TRPC5- and TRPC6-overexpressing cells, the corresponding murine cDNAs were subcloned into bicistronic pIRESneo vectors (Clontech, Palo Alto, CA) and then transfected into HEK293 or Jurkat T cells using Lipofectamine 2000 (Invitrogen, Carlsbad, CA) following the manufacturer's protocol. The transfected cells were grown in the aforementioned media supplemented with G418 (400 μg/mL and 1 mg/mL for HEK293 and Jurkat T cells, respectively) for 3 weeks to establish the polyclonal stable cell lines. All stable cell lines were maintained with the presence of G418 in the culture medium. Cells were passaged at 1:4 dilution with fresh medium once every 4 days.

Western Blot Analysis. Collected cells were suspended in phosphate-buffered saline (PBS) with 0.5% Lubrol. After brief sonication, the mixture was centrifuged at 1500*g* for 5 min, and the supernatant was preserved for analysis. Amounts of total protein were analyzed by a protein assay kit (Bio-Rad, Hercules, CA). Fifty micrograms of total protein was separated by SDS−PAGE and transferred to a nitrocellulose membrane using a semidry transfer cell. After being blocked with Tris-buffered saline with 0.1% Tween 20 (TBST) containing 5% nonfat milk for 60 min, the transblotted membrane was incubated with the primary antibody at the appropriate dilution (1:1000) in TBST, and 5% nonfat milk at 4 °C overnight. After being washed with TBST for 15 min three times, the membrane was incubated with 1:4000 diluted goat anti-rabbit or goat anti-mouse IgG−horseradish peroxidase conjugates (Jackson Labs, West Grove, PA) at room temperature for 1 h. After being washed with TBST three times, the immunoblots were visualized by enhanced chemiluminescence.

Ligand Binding Assays. Wild-type and individual TRPC-overexpressing HEK293 cells (1×10^6 cells) were suspended in 0.5 mL of binding assay buffer (100 mM KCl, 2 mM $MgCl_2$, 0.5% Lubrol, and 20 mM Tris-HCl, pH 7.5) in the presence of 1% protease inhibitor cocktail (Calbiochem, San Diego, CA). After brief sonication, cell lysates were centrifuged at 1500*g* for 5 min. The supernatant was collected and incubated with 40 μM biotin-PIP_3 or biotin-PIP_2 at 4 °C for 12 h, followed by 50 μL of streptavidin beads (Sigma, St. Louis, MO). The mixture was incubated for an additional 2 h and centrifuged at 12000*g* for 5 min. The collected beads were washed with 1 mL of binding assay buffer three times, and the bound proteins were subjected to Western blot analysis.

Fluorescence Spectrophotometric Measurement of $[Ca^{2+}]_i$ Response. $[Ca^{2+}]_i$ was measured by using Fura-2 fluorometry.

Cells (2.5×10^6 cells/mL) were loaded with 2 μM Fura-2/AM in the presence of 2 mM probenecid in DMEM medium in the dark at 37 °C for 1.5 h. The loaded cells were centrifuged at 1000*g* for 5 min, washed twice with Ca^{2+} assay buffer (4.3 mM Na_2HPO_4, 24.3 mM NaH_2PO_4, 4.3 mM K_2HPO_4, 113 mM NaCl, and 5 mM glucose, pH 7.4), and resuspended in the same buffer (2.5×10^5 cells/mL) with or without 1 mM Ca^{2+}. Fura-2 fluorescence was monitored by a Hitachi F2500 spectrofluorometer at 37 °C with excitation at 340 and 380 nm and emission at 510 nm, and the ratio of F_{340}/F_{380} (R) was recorded. The maximum fluorescence ratio (R_{max}) was determined by adding 0.1% Triton X-100, and the minimum fluorescence ratio (R_{min}) was determined following depletion of external Ca^{2+} by adding 5 mM EGTA. $[Ca^{2+}]_i$ was calculated according to the equation $[Ca^{2+}]_i = K_d(Sf_2/Sb_2)(R - R_{min})/(R_{max} - R)$, where K_d (224 nM) is the dissociation constant for Ca^{2+} and Sf_2 and Sb_2 denote emission fluorescence values obtained from 380 nm excitation at minimum and maximum ratio, respectively.

Ratiometric Digital Imaging of $[Ca^{2+}]_i$. Cells (1×10^5/coverslip) were seeded on round (25 mm) glass coverslips and cultured in DMEM medium supplemented with 10% FBS at 37 °C in a humidified incubator (5% CO_2). Before each experiment, the cells were loaded with 2 μM Fura-2/AM in the aforementioned assay buffer in the presence of 0.5% bovine serum albumin and 2 mM probenecid in the dark for 1.5 h at 37 °C. The cells were washed twice with assay buffer to finish the loading procedure. Coverslips with Fura-2-loaded cells were placed in a chamber (Molecular Probes, Eugene, OR) and covered with 500 μL of assay buffer containing 1 mM Ca^{2+}. Cells were imaged using a Nikon inverted microscope equipped with a CCD camera (CoolSnap HQ) and a 40× lens. Images were acquired alternately every 1 s from excitation at 340 and 380 nm and emission at 510 nm and analyzed using MetaFluor software (Universal Imaging, Downingtown, PA). Regions of interest containing 10−20 cells were isolated, and the fluorescence intensity ratios at 340 and 380 nm were averaged.

Measurement of Intracellular IP_3 Production. Analysis of agonist-stimulated IP_3 production was carried out by using a Biotrak IP_3 assay kit (Amersham Biosciences, Piscatway, NJ), in which unlabeled IP_3 competes with a fixed amount of $[^3H]IP_3$ for a limited number of bovine adrenal IP_3 binding proteins. TRPC6-overexpressed HEK293 cells (2×10^5) suspended in 0.4 mL of the aforementioned Ca^{2+} assay buffer were used for each assay. After being treated with PIP_3 or carbachol for various time intervals, intracellular IP_3 was extracted by treating cells with perchloric acid. In brief, 0.2 volume of ice-cold 20% perchloric acid was added to the cell suspension, and the resultant mixture was incubated on ice for 20 min. The mixture was centrifuged at 2000*g* at 4 °C for 15 min, and the supernatant was transferred to another tube. After the supernatant was neutralized by ice-cold 10 M KOH to pH 7.5 and the $KClO_4$ was removed by centrifugation at 2000*g* at 4 °C for 15 min, 100 μL of supernatant was used for IP_3 analysis according to the manufacturer's instruction.

Antisense Oligonucleotide Transfection. Transfection of Jurkat T cells with the antisense oligonucleotide for TRPC6, TTGGCCCTTGCAAACTTCCACTCCA (*22*, *23*), was carried out according to the manufacturer's instruction. In brief, the oligonucleotide in 1 mL of serum-free Opti-MEM medium was mixed with 15 μL of Lipofectamine 2000 reagent (Invitrogen, Carlsbad, CA) at room temperature for 30 min and added to 5×10^6 Jurkat cells suspended in 4 mL of serum-free Opti-MEM medium. After 5 h at 37 °C, the transfection medium was replaced with 5 mL of 10% FBS-containing RPMI 1640 medium. The transfected cells were allowed to grow for an additional 24 h before experiments.

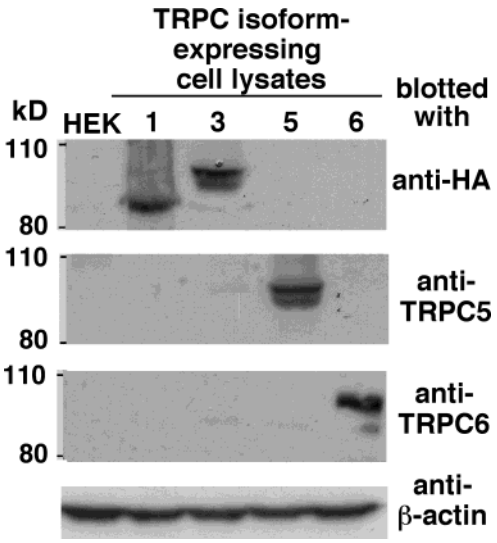

FIGURE 1: Western blots demonstrating the expression of TRPC proteins in the respective stable clones. Since TRPC1 and TRPC3 contained an HA tag at the N- and C-termini, respectively, they were blotted with anti-HA antibodies. TRPC5 and TRPC6 were analyzed with the respective antibodies.

RT-PCR Analysis of mRNA Transcripts of the TRPC6 Gene. Jurkat T cells (1×10^7 cells) were subjected to total RNA isolation by using a RNeasy mini kit (Qiagen, Valenia, CA). RNA concentration and quality were assessed spectophotometrically by measuring absorbance at 260 and 280 nm. RNA (2 μg) was reverse-transcribed to cDNA by using an Omniscript RT kit (Qiagen), followed by PCR amplification. The primers used were as follows: TRPC6, forward, 5′-AAAGATATCTTCAAATTCATGGTC-3′, and reverse, 5′-CACATCCGCATCATCCTCAATTTC-3′; β-actin, forward, 5′-TCTACAATGAGCTG-CGTGTG-3′, and reverse, 5′-GGTCAGGATCTTCATGAGGT-3′. The PCR products were analyzed on 1.2% agarose gels and visualized by ethidium bromide staining.

RESULTS

Stable HEK293 Cell Lines Expressing TRPC1, TRPC3, TRPC5, and TRPC6. To investigate the role of PIP_3 in TRPC activation, we developed stable HEK293 cell lines expressing TRPC isoforms 1, 3, 5, and 6, among which TRPC1 and TRPC3 contained a hemagglutinin (HA) tag at the N- and C-termini, respectively. Figure 1 depicts the immunoblots of cell lysates from HEK293 and individual cell lines using antibodies against HA and TRPC isoforms 5 and 6 accordingly.

As shown, each stable cell line expressed relatively high levels of the respective TRPC isoform, while the expression of any of these TRPC proteins was undetectable in the parental HEK cells. The presence of multiple protein bands with TRPC3 and TRPC5 might be due to differences in the

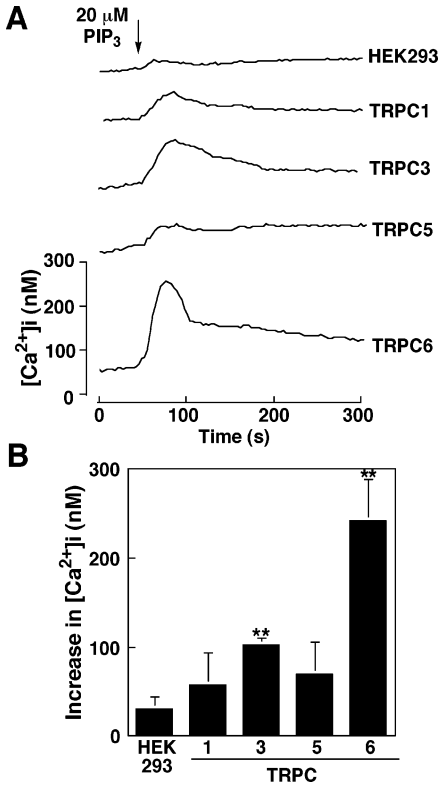

FIGURE 2: PIP_3 activates intracellular Ca^{2+} increases in TRPC6-expressing cells. (A) Effect of PIP_3 (20 μM) on $[Ca^{2+}]_i$ in HEK293 and individual TRPC-expressing cells. $[Ca^{2+}]_i$ was measured by Fura-2 fluorometry as described under Experimental Procedures. PIP_3 was introduced at the time indicated by the arrow. Traces are representative of five independent experiments. (B) Mean amplitudes of PIP_3-induced Ca^{2+} response in control and individual TPRC-expressing cells ($n = 5$). The amplitudes were obtained by subtracting the baseline from the highest point of $[Ca^{2+}]_i$. The double asterisk (**) indicates the statistical significance of $p < 0.001$, compared with the control (by Student's t test).

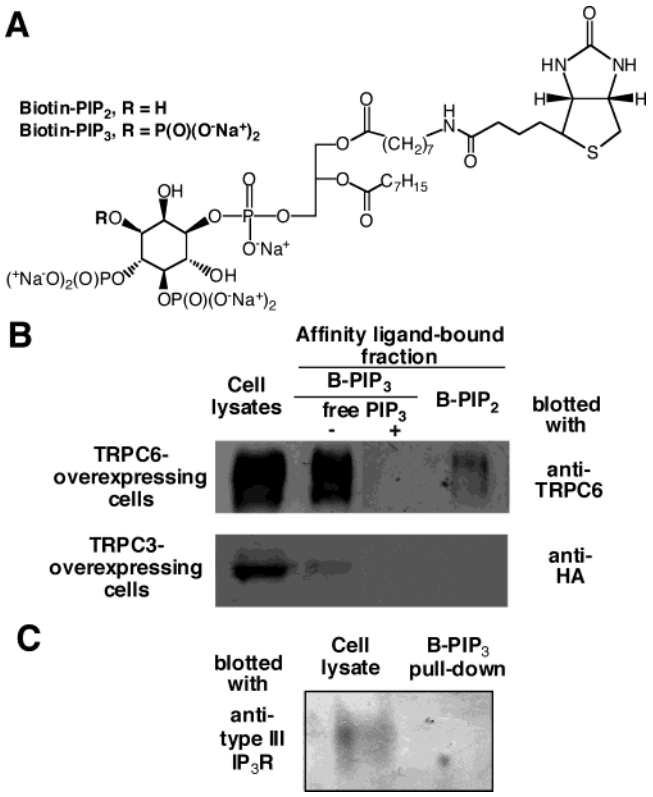

FIGURE 3: Selective interactions between biotin-PIP_3 and TRPC6. (A) Structures of biotin-PIP_2 and biotin-PIP_3. (B) Pull-down analysis using biotin-PIP_3 and biotn-PIP_2 with lysates from TRPC6- (upper panel) and TRPC3-overexpressing (lower panel) cells. Cell lysates from individual cell lines were exposed to biotin-PIP_3 (denoted by B-PIP_3; 40 μM), in the absence (−) or presence (+) of di-C_8-PIP_3 (100 μM), or biotin-PIP_2 (denoted by B-PIP_2; 40 μM), followed by streptavidin beads. Cell lysates (from left, lane 1) and the affinity ligand-purified proteins (lanes 2−4) were analyzed by Western blot analysis using the respective antibodies. The amounts of cell lysates loaded onto the gel represented $^1/_{20}$th of that used for the pull-down assay. (C) Lack of IP_3R proteins in the biotin-PIP_3-bound fraction. Cell lysates from TRPC6-overexpressing cells and the biotin-PIP_3 pull-down fraction were probed by anti-type III IP_3R antibodies.

extent of glycosylation during remodeling of the protein-attached sugar moieties (*21*).

Effect of PIP_3 on $[Ca^{2+}]_i$ in Stable HEK Cell Lines Expressing Different TRPC Channels. Published data from this and other laboratories have shown that PIP_3 and other inositol lipids are cell-permeant and can readily fuse with cell membranes to exert cellular responses in different types of cells, including platelets (*10*), NIH3T3 cells (*24*), adipocytes (*25*), Jurkat T cells (*11*), and RBL-2H3 mast cells (*12*). Thus, we examined the Ca^{2+}-perturbing effect of exogenous PIP_3 on HEK293 and its stable cell lines expressing individual TRPC channels by using Fura-2 spectrofluorometry. Figure 2A shows traces representative of $[Ca^{2+}]_i$ responses to 20 μM micellar PIP_3 in HEK293 and its stable cell lines expressing TRPC1, TRPC3, TRPC5, and TRPC6. Relatively, the extent of Ca^{2+} responses to PIP_3 was in the order of TRPC6 ≫ TRPC3 ≫ TRPC1, TRPC5, and HEK293 (Figure 2B).

As shown, PIP_3 induced marginal, yet appreciable, $[Ca^{2+}]_i$ increase in HEK293 parent cells. As PIP_3 does not perturb the permeability of lipid membranes to Ca^{2+} (*11*), this small increase might be attributable to the presence of low levels of PIP_3-sensitive Ca^{2+} entry in HEK cells. While Ca^{2+} responses to PIP_3 in TRPC1- and TPRC-5-expressing cells were not statistically different from that of PIP_3-stimulated HEK293 cells ($p > 0.2$), the amplitude of Ca^{2+} changes in TRPC6 and TRPC3 cells, especially the former, was significantly higher than that of the parent cells ($p < 0.001$).

Interactions of PIP_3 with TRPC6 and TRPC3. To confirm the selective effect of PIP_3 on TRPC6 and TRPC3, we used biotinylated PIP_3 and PIP_2 analogues (Figure 3A) to assess the physical interactions of PIP_3 with these two TRPC proteins. The biotin-PIP_3 affinity ligand has been successfully applied to the purification of PIP_3 binding proteins (*11*). Lysates of each of the TRPC cells were exposed to biotin-PIP_3 (40 μM) with or without the presence of competing free di-C_8-PIP_3 (100 μM), followed by streptavidin beads. In addition, biotin-PIP_2 (40 μM) was used to examine the specificity of this phosphoinositide binding. Binding of individual TRPC isoforms to the affinity ligand was analyzed by Western blotting as aforementioned (Figure 3B).

As expected, TRPC6 and, to a lesser extent, TRPC3 displayed specific binding to biotin-PIP_3 as the binding could be abrogated by competing di-C_8-PIP_3. A low level of TRPC6 binding to biotin-PIP_2 was noted, which, however, accounted for less than 5% of that of biotin-PIP_3. This differential recognition indicates a high degree of ligand specificity despite the largely shared structural motifs

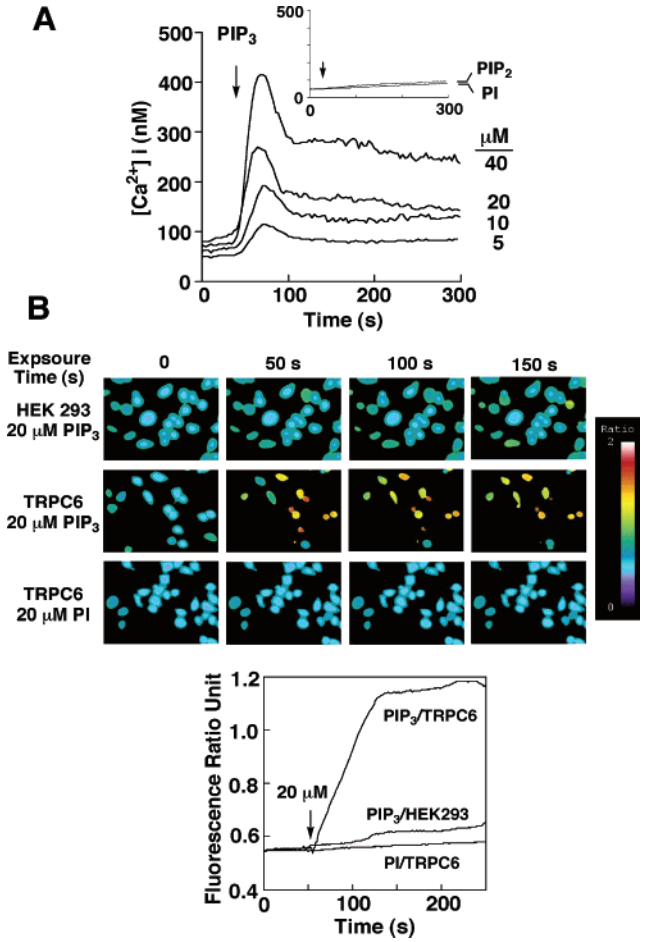

FIGURE 4: Dose dependency and specificity of PIP_3-induced Ca^{2+} response in TRPC6-expressing HEK293 cells. (A) Time course and dose dependence of the effect of PIP_3 on $[Ca^{2+}]_i$ in TRPC6 cells. Inset: PIP_2 and PI, 20 μM each, had no effect on $[Ca^{2+}]_i$ in TRPC6 cells. The arrows indicate the time of addition of individual compounds. (B) Upper panel: Digital ratiometric imaging analysis of the Ca^{2+} response to 20 μM PIP_3 and/or PI in HEK and TRPC6 cells. Shown are pseudocolor images taken at 50 s intervals posttreatment. Lower panel: Time course of Ca^{2+} responses based on the above ratiometric imaging analysis.

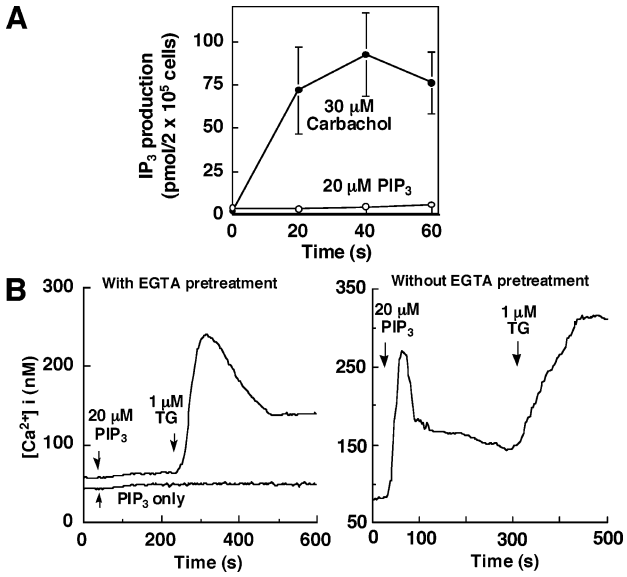

FIGURE 5: PIP_3-mediated Ca^{2+} response in TRPC6 cells is independent of PLC and internal Ca^{2+} stores. (A) Effect of PIP_3 and carbachol on IP_3 production in TRPC6 cells. TRPC6-overexpressing HEK293 cells (2×10^5) were exposed to PIP_3 (20 μM) or carbachol (30 μM), and agonist-stimulated IP_3 production was analyzed by using a Biotrak IP_3 assay kit as described in Experimental Procedures. Each data point represents the mean $\pm$ SD ($n = 5$). (B) PIP_3 does not affect thapsigargin-sensitive internal Ca^{2+} pools in TRPC6 cells in either the absence (left panel) or presence of external Ca^{2+}. Fura-2-loaded TRPC6 cells, in the presence or absence of 5 mM EGTA, were treated with, in tandem, 20 μM PIP_3 and 1 μM thapsigargin, at time points indicated by arrows.

between PIP_3 and PIP_2. Together with the differential Ca^{2+} responses, these data indicate that PIP_3 selectively interacts with TRPC6 and, to a lesser extent, its close homologue TRPC3. Moreover, in light of the recent report that inositol 1,4,5-trisphosphate receptors (IP_3Rs) interact and activate TRPC channels (*26*), we also probed the biotin-PIP_3-bound fraction vis-à-vis cell lysates with anti-type III IP_3R antibodies. Although the cell lysates contained detectable amounts of IP_3Rs, no IP_3R binding could be detected in association with the biotin-PIP_3-bound fraction (Figure 3C).

To shed light onto the role of PIP_3 in TRPC channel activation, we further characterized PIP_3-induced Ca^{2+} perturbation in TRPC6-expressing cells.

PIP_3-Stimulated Ca^{2+} Perturbation in TRPC6-Expressing HEK293 Cells Is Specific. Fura-2 fluorometric analysis indicates that the effect of PIP_3 on $[Ca^{2+}]_i$ in TRPC6 cells was dose-dependent and highly structurally specific (Figure 4A). The response to exogenous micellar PIP_3 was appreciable at as low as 5 μM and reached a plateau at approximately 40 μM. Exposure to other phosphoinositides such as PIP_2 and phosphatidylinositol (PI) failed to give rise to significant Ca^{2+} responses (Figure 4A, inset). This stringent phosphoinositide specificity in Ca^{2+} perturbation underscores the role of PIP_3 as a second messenger in Ca^{2+} signaling through TRPC6 activation.

PIP_3-induced Ca^{2+} changes in Fura-2-loaded cells were also monitored by digital ratiometric imaging (Figure 4B). These pseudocolor images demonstrate a time-dependent $[Ca^{2+}]_i$ response to PIP_3 (20 μM) in TRPC6 cells, while no appreciable effect was noted with PI. In parental HEK293 cells, PIP_3-elicted Ca^{2+} perturbation was minimal vis-à-vis that of TRPC6 cells.

PIP_3-Mediated Ca^{2+} Response in TRPC6-Expressing HEK293 Cells Is Independent of PLC. A crucial issue that warranted clarification was the role of PLC in the PIP_3-mediated Ca^{2+} response since PIP_3 at high concentrations (>50 μM) has been shown to stimulate IP_3 production via PLCγ activation (*27*, *28*). To discern the involvement of PLC, we examined intracellular IP_3 production in response to PIP_3 (20 μM) vis-à-vis carbachol (30 μM) in TRPC6 cells. Carbachol, a cholingeric agonist, is well-known to activate IP_3 production, leading to $[Ca^{2+}]_i$ increase (*29*). Figure 5A indicates that while carbachol induced a robust increase in IP_3 levels, intracellular IP_3 remained virtually unaltered after treatment of 20 μM PIP_3, suggesting that PLC was not activated.

We further obtained evidence that this PIP_3-elicited Ca^{2+} perturbation in TRPC6-expressing cells was mediated through store-independent, nonselective cation channels, which are characteristics of TRPC6. To confirm that this Ca^{2+} increase was independent of internal Ca^{2+} stores, TRPC6 cells were treated with 20 μM PIP_3 followed by exposure to thapsigargin in the absence or presence of external Ca^{2+} (Figure

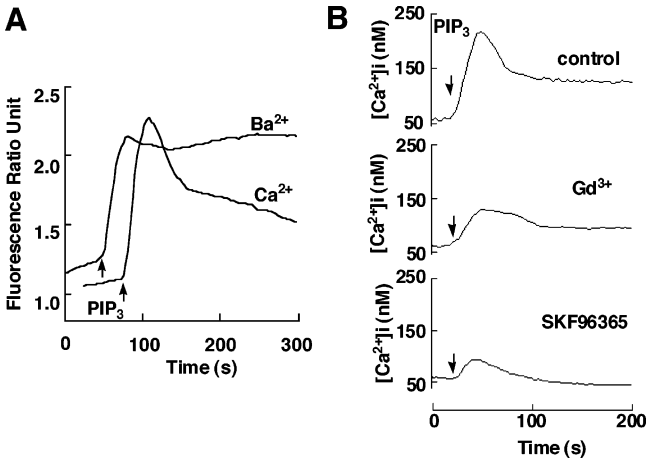

FIGURE 6: PIP_3 mediates Ca^{2+} entry via a nonselective cation channel, which is sensitive to known TRPC6 inhibitors. (A) Ba^{2+} and Ca^{2+} response to PIP_3 in TRPC6 cells. Fura-2-loaded TRPC6 cells, in the presence of 1 mM Ba^{2+} or Ca^{2+}, were exposed to 20 μM PIP_3, and the increase in fluorescence ratio (340:380 nm) was recorded. The arrows indicate the time of addition of individual compounds. (B) Ca^{2+} response to 20 μM PIP_3 in the presence of 50 μM Gd^{3+} and 10 μM SKF96365.

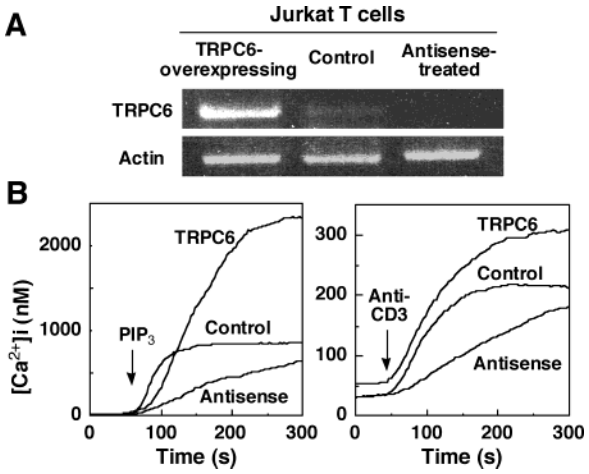

FIGURE 7: Effect of TRPC6 expression levels on PIP_3- and anti-CD3-activated Ca^{2+} response in Jurkat T cells. (A) RT-PCR analysis of mRNA levels of TRPC6 in TRPC6-overexpressing Jurkat T cells (from left, lane 1), normal Jurkat T cells (lane 2), and Jurkat T cells treated with TRPC6 antisense oligonucleotide (lane 3). (B) The amplitude of the Ca^{2+} response to PIP_3 (left panel) and anti-CD3 (right panel) in Jurkat T cells is affected by TRPC expression. TRPC6-overexpressing (TRPC6), normal, and antisense oligonucleotide-treated Jurkat T cells were loaded with Fura-2 and exposed to 20 μM PIP_3 or 10 μg/mL anti-CD3 in the presence of 1 mM Ca^{2+}, and the increase in fluorescence ratio (340:380 nm) was recorded. The arrows indicate the time of addition of individual compounds.

5B). As shown, EGTA pretreatment completely abrogated PIP_3-triggered Ca^{2+} increase, and PIP_3 exposure did not affect the extent of thapsigargin-induced Ca^{2+} response in the Ca^{2+}-depleted milieu (left panel). Meanwhile, treatment of TRPC6 cells with PIP_3 (20 μM) in the presence of external Ca^{2+} did not hamper the ability of thapsigargin (1 μM) to perturb $[Ca^{2+}]_i$ (right panel), suggesting that the integrity of internal Ca^{2+} stores was not affected by PIP_3.

With regard to cation selectivity, PIP_3 (20 μM) stimulated the entry of both Ca^{2+} and Ba^{2+} in TRPC6 cells at comparable rates (Figure 6A). This finding is consistent with the nonselective nature of TRPC6 in cation entry. It is noteworthy that the kinetics of Ba^{2+} entry differed from that of Ca^{2+}; i.e., intracellular Ba^{2+} levels increased to a plateau while that of Ca^{2+} was transient, consistent with Ba^{2+} being a poor substrate for plasma membrane Ca^{2+} pumps (*30*). In addition, PIP_3-mediated Ca^{2+} entry in TRPC6 cells could be blocked by a number of known inhibitors for TRPC6 (Figure 6B) including Gd^{3+} (50 μM) and SKF96365 (10 μM).

Role of TRPC6 in PIP_3- and Anti-CD3-Mediated Ca^{2+} Response in Jurkat T Cells. The link between TRPC6 and PIP_3-induced Ca^{2+} entry provided a molecular basis to account for the role in PI3K in receptor-activated Ca^{2+} influx in Jurkat T cells and RBL-2H3 mast cells (*11*, *12*). Accordingly, we examined the effect of modulating the level of TRPC6 on PIP_3- and anti-CD3-induced Ca^{2+} response in Jurkat T cells. First, we stably transfected Jurkat T cells with a TRPC6 construct. RT-PCR analysis indicates that Jurkat T cells expressed low, yet detectable, levels of TRPC6 mRNA, and a substantial increase in the mRNA transcript of the *TRPC6* gene was noted in these TRPC6-overexpressing Jurkat T cells (Figure 7A). As shown, exposure of these cells to either PIP_3 (20 μM) or anti-CD3 (10 μg/mL) gave rise to more robust Ca^{2+} response as compared to Jurkat T cells (Figure 7B: left panel, PIP_3 treatment; right panel, anti-CD3 treatment). In addition, we used a TRPC6 antisense oligonucleotide (TTGGCCCTTGCAAACTTCCA-CTCCA) (*22*, *23*) to inhibit TRPC6 expression in Jurkat T cells (Figure 7A). As expected, decreased TRPC6 expression significantly reduced the amplitude of Ca^{2+} response to PIP_3 and anti-CD3. Together, these data support the premise that TRPC6 played a role in PIP_3- and receptor-activated Ca^{2+} entry in Jurkat T cells.

DISCUSSION

Using Jurkat T cells and RBL-2H3 cells, we previously demonstrated that PI3K facilitated agonist-stimulated Ca^{2+} influx through a PIP_3-sensitive Ca^{2+} entry mechanism (*11*, *12*). This unique PIP_3-mediated Ca^{2+} transport has also been shown to be involved in platelet aggregation (*10*). Given the intimate relationship between PI3K and PLCγ in receptor tyrosine kinase signaling, we hypothesize that PIP_3, the primary output signal of PI3K, can generate Ca^{2+} stimuli via a store-independent mechanism that synergizes with IP_3-induced Ca^{2+} release and capacitative Ca^{2+} entry for sustaining elevated $[Ca^{2+}]_i$, a driving force underlying many cellular responses in these hematopoietic cells.

To date, the molecular identity of this novel PIP_3-sensitive Ca^{2+} entry system has not been identified. The present study focused on a potential link between PIP_3-induced Ca^{2+} entry and TRPC channels, of which the rationale was twofold. First, TRPC channels are ubiquitously expressed in Jurkat T cells, RBL2H3 mast cells, and platelets (*13*, *14*, *31*, *32*). Second, the regulation of many of these TRP channels remains elusive. By expressing TRPC isoforms in HEK293 cells, we obtain two lines of evidence that PIP_3 activates TRPC6 and, to a lesser extent, its subfamily member TRPC3. First, fluorometric Ca^{2+} measurement demonstrated the ability of PIP_3 to selectively stimulate $[Ca^{2+}]_i$ increase in TRPC6 cells. Although this PIP_3-mediated Ca^{2+} perturbation was also noted in TRPC3 cells, the level of $[Ca^{2+}]_i$ increase was approximately 30% of that in TRPC6. Second, pull-down analysis indicates that biotin-PIP_3 could interact with

TRPC6 in a specific manner as the binding could be displaced by free di-C_8-PIP_3. Although a similar pull-down analysis was carried out in Jurkat T cells to study PIP_3 binding proteins, proteins with molecular mass similar to that of TRPC6 were not noted (*11*), in part due to the extremely low abundance of TRPC6 channels in plasma membranes.

Our data indicate that PIP_3 activates store-independent Ca^{2+} entry in TRPC6 cells via a nonselective cation channel. Known inhibitors of TRPC6, such as Gd^{3+} and SKF96365, could inhibit this PIP_3-activated Ca^{2+} entry. In addition, exposure of TRPC6 cells to PIP_3 did not give rise to IP_3 production, excluding the involvement of PLCγ and internal stores in the consequent $[Ca^{2+}]_i$ increase. The activating effect of PIP_3 on TRPC6 is reminiscent to that of OAG (*6*) but is distinct from that of HETE since HETE did not provoke changes in intracellular Ca^{2+} (*16*). Although the structure of PIP_3 encompasses a DAG moiety, the PIP_3 effect was unlikely attributable to the DAG substructure in light of the phosphoinositide specificity in TRPC6 activation; i.e., PIP_2 and PI were ineffective in triggering Ca^{2+} responses. It is plausible that both lipid mediators activate TRPC6 through different binding sites, which underscores our hypothesis that PI3K and PLCγ play concerted, yet mechanistically distinct roles in triggering Ca^{2+} response to receptor tyrosine kinase activation.

TRPC6 has been shown to constitute a store-independent cation channel in various cell systems, including human platelet (*13*), Jurkat T cells (*14*), and A7r5 smooth muscle cells (*22*). The putative link between TRPC6 and PIP_3-induced Ca^{2+} entry provides a molecular basis to account for the role of PI3K in the regulation of receptor-activated Ca^{2+} response in these cells. Consequently, TRPC6 not only provides molecular insight into the physiological role of PI3K in the activation of leukocytes and platelets but may also be pharmacologically exploited as a therapeutic target for diseases relevant to these blood cells (*32*). For example, using Jurkat T cells, we demonstrated that the amplitude of PIP_3- and, more importantly, anti-CD3-mediated Ca^{2+} response could be altered by modulating the level of TRPC6 expression. Thus, design of specific inhibitors of this Ca^{2+} channel is of translational relevance. In addition, examinations of the involvement of TRPC6 in PI3K-mediated Ca^{2+} entry in other cell systems are currently under way.

ACKNOWLEDGMENT

The authors thank Ms. Dina Chuang-Zhu for technical assistance in establishing and maintaining the stable cell lines.

REFERENCES

1. Montell, C., Birnbaumer, L., Flockerzi, V., Bindels, R. J., Bruford, E. A., Caterina, M. J., Clapham, D. E., Harteneck, C., Heller, S., Julius, D., Kojima, I., Mori, Y., Penner, R., Prawitt, D., Scharenberg, A. M., Schultz, G., Shimizu, N., and Zhu, M. X. (2002) A unified nomenclature for the superfamily of TRP cation channels, *Mol. Cell 9*, 229−231.
2. Montell, C., Birnbaumer, L., and Flockerzi, V. (2002) The TRP channels, a remarkably functional family, *Cell 108*, 595−598.
3. Trebak, M., Vazquez, G., Bird, G. S., and Putney, J. W., Jr. (2003) The TRPC3/6/7 subfamily of cation channels, *Cell Calcium 33*, 451−461.
4. Liu, X., Wang, W., Singh, B. B., Lockwich, T., Jadlowiec, J., O'Connell, B., Wellner, R., Zhu, M. X., and Ambudkar, I. S. (2000) Trp1, a candidate protein for the store-operated Ca(2+) influx mechanism in salivary gland cells, *J. Biol. Chem. 275*, 3403−3411.
5. Vazquez, G., Wedel, B. J., Trebak, M., Bird, St. J. G., and Putney, J. W., Jr. (2003) Expression level of the canonical transient receptor potential 3 (TRPC3) channel determines its mechanism of activation, *J. Biol. Chem. 278*, 21649−21654.
6. Hofmann, T., Obukhov, A. G., Schaefer, M., Harteneck, C., Gudermann, T., and Schultz, G. (1999) Direct activation of human TRPC6 and TRPC3 channels by diacylglycerol, *Nature 397*, 259−263.
7. Kiselyov, K., Xu, X., Mozhayeva, G., Kuo, T., Pessah, I., Mignery, G., Zhu, X., Birnbaumer, L., and Muallem, S. (1998) Functional interaction between InsP3 receptors and store-operated Htrp3 channels, *Nature 396*, 478−482.
8. Boulay, G., Brown, D. M., Qin, N., Jiang, M., Dietrich, A., Zhu, M. X., Chen, Z., Birnbaumer, M., Mikoshiba, K., and Birnbaumer, L. (1999) Modulation of Ca(2+) entry by polypeptides of the inositol 1,4,5-trisphosphate receptor (IP3R) that bind transient receptor potential (TRP): evidence for roles of TRP and IP3R in store depletion-activated Ca(2+) entry, *Proc. Natl. Acad. Sci. U.S.A. 96*, 14955−14960.
9. Zhang, Z., Tang, J., Tikunova, S., Johnson, J. D., Chen, Z., Qin, N., Dietrich, A., Stefani, E., Birnbaumer, L., and Zhu, M. X. (2001) Activation of Trp3 by inositol 1,4,5-trisphosphate receptors through displacement of inhibitory calmodulin from a common binding domain, *Proc. Natl. Acad. Sci. U.S.A. 98*, 3168−3173.
10. Lu, P.-J., Hsu, A.-L., Wang, D.-S., and Chen, C.-S. (1998) Phosphatidylinositol 3,4,5-trisphosphate triggers platelet aggregation by activating Ca^{2+} influx, *Biochemistry 37*, 9776−9783.
11. Hsu, A.-L., Ching, T.-T., Sen, G., Wang, D.-S., Bondada, S., Authi, K. S., and Chen, C.-S. (2000) Novel function of phosphoinositide 3-kinase in T cell Ca^{2+} signaling. A phosphatidylinositol 3,4,5-trisphosphate-mediated Ca^{2+} entry mechanism, *J. Biol. Chem. 275*, 16242−16250.
12. Ching, T.-T., Hsu, A.-L., Johnson, A. J., and Chen, C.-S. (2001) Phosphoinositide 3-kinase facilitates antigen-stimulated Ca(2+) influx in RBL-2H3 mast cells via a phosphatidylinositol 3,4,5-trisphosphate-sensitive Ca(2+) entry mechanism, *J. Biol. Chem. 276*, 14814−14820.
13. Hassock, S. R., Zhu, M. X., Trost, C., Flockerzi, V., and Authi, K. S. (2002) Expression and role of TRPC proteins in human platelets: evidence that TRPC6 forms the store-independent calcium entry channel, *Blood 100*, 2801−2811.
14. Gamberucci, A., Giurisato, E., Pizzo, P., Tassi, M., Giunti, R., McIntosh, D. P., and Benedetti, A. (2002) Diacylglycerol activates the influx of extracellular cations in T-lymphocytes independently of intracellular calcium-store depletion and possibly involving endogenous TRP6 gene products, *Biochem. J. 364*, 245−254.
15. Pizzo, P., Burgo, A., Pozzan, T., and Fasolato, C. (2001) Role of capacitative calcium entry on glutamate-induced calcium influx in type-I rat cortical astrocytes, *J. Neurochem. 79*, 98−109.
16. Basora, N., Boulay, G., Bilodeau, L., Rousseau, E., and Payet, M. D. (2003) 20-hydroxyeicosatetraenoic acid (20-HETE) activates mouse TRPC6 channels expressed in HEK293 cells, *J. Biol. Chem. 278*, 31709−31716.
17. Watanabe, H., Vriens, J., Prenen, J., Droogmans, G., Voets, T., and Nilius, B. (2003) Anandamide and arachidonic acid use epoxyeicosatrienoic acids to activate TRPV4 channels, *Nature 424*, 434−438.
18. Runnels, L. W., Yue, L., and Clapham, D. E. (2002) The TRPM7 channel is inactivated by PIP(2) hydrolysis, *Nat. Cell Biol. 4*, 329−336.
19. Kawanabe, Y., Hashimoto, N., and Masaki, T. (2002) Effects of phosphoinositide 3-kinase on the endothelin-1-induced activation of voltage-independent Ca(2+) channels and mitogenesis in Chinese hamster ovary cells stably expressing endothelin(a) receptor, *Mol. Pharmacol. 62*, 756−761.
20. Wang, D.-S., Ching, T.-T., St Pyrek, J., and Chen, C.-S. (2000) Biotinylated phosphatidylinositol 3,4,5-trisphosphate as affinity ligand. *Anal. Biochem. 280*, 301−307.
21. Zhu, X., Jiang, M., and Birnbaumer, L. (1998) Receptor-activated Ca^{2+} influx via human Trp3 stably expressed in human embryonic kidney (HEK)293 cells. Evidence for a noncapacitative Ca^{2+} entry, *J. Biol. Chem. 273*, 133−142.
22. Jung, S., Strotmann, R., Schultz, G., and Plant, T. D. (2002) TRPC6 is a candidate channel involved in receptor-stimulated cation currents in A7r5 smooth muscle cells, *Am. J. Physiol. Cell. Physiol. 282*, C347−C359.

23. Yu, Y., Sweeney, M., Zhang, S., Platoshyn, O., Landsberg, J., Rothman, A., and Yuan, J. X. (2003) PDGF stimulates pulmonary vascular smooth muscle cell proliferation by upregulating TRPC6 expression, *Am. J. Physiol. Cell. Physiol. 284*, C316−C330.
24. Derman, M. P., Toker, A., Hartwig, J. H., Spokes, K., Falck, J. R., Chen, C.-S., Cantley, L. C., and Cantley, L. G. (1997) The lipid products of phosphoinositide 3-kinase increase cell motility through protein kinase C, *J. Biol. Chem. 272*, 6465−6470.
25. Gagnon, A., Chen, C.-S., and Sorisky, A. (1999) Activation of protein kinase B and induction of adipogenesis by insulin in 3T3-L1 preadipocytes: contribution of phosphoinositide-3,4,5-trisphosphate versus phosphoinositide-3,4-bisphosphate, *Diabetes 48*, 691−698.
26. Zhu, M. X., and Tang, J. (2004) TRPC channel interactions with calmodulin and IP3 receptors, *Novartis Found. Symp. 258*, 44−58.
27. Bae, Y. S., Cantley, L. G., Chen, C.-S., Kim, S. R., Kwon, K. S., and Rhee, S. G. (1998) Activation of phospholipase C-gamma by phosphatidylinositol 3,4,5-trisphosphate, *J. Biol. Chem. 273*, 4465−4469.
28. Barker, S. A., Caldwell, K. K., Pfeiffer, J. R., and Wilson, B. S. (1998) Wortmannin-sensitive phosphorylation, translocation, and activation of PLCgamma1, but not PLCgamma2, in antigen-stimulated RBL-2H3 mast cells, *Mol. Biol. Cell 9*, 483−496.
29. Marc, S., Leiber, D., and Harbon, S. (1986) Carbachol and oxytocin stimulate the generation of inositol phosphates in the guinea pig myometrium, *FEBS Lett. 201*, 9−14.
30. Schilling, W. P., Rajan, L., and Strobl-Jager, E. (1989) Characterization of the bradykinin-stimulated calcium influx pathway of cultured vascular endothelial cells. Saturability, selectivity, and kinetics, *J. Biol. Chem. 264*, 12838−12848.
31. Garcia, R. L., and Schilling, W. P. (1997) Differential expression of mammalian TRP homologues across tissues and cell lines, *Biochem. Biophys. Res. Commun. 239*, 279−283.
32. Li, S. W., Westwick, J., and Poll, C. T. (2002) Receptor-operated Ca^{2+} influx channels in leukocytes: a therapeutic target?, *Trends Pharmacol. Sci. 23*, 63−70.

BI049349F